

See discussions, stats, and author profiles for this publication at: <https://www.researchgate.net/publication/229423195>

Quantum-mechanical Studies on the Origin of Barriers to Internal Rotation about Single Bonds

ARTICLE *in* JOURNAL OF THE AMERICAN CHEMICAL SOCIETY · MARCH 1979

Impact Factor: 12.11 · DOI: 10.1021/ja00501a009

CITATIONS

276

READS

37

2 AUTHORS, INCLUDING:



Frank Weinhold

University of Wisconsin-Madison

199 PUBLICATIONS 28,872 CITATIONS

SEE PROFILE

Quantum-Mechanical Studies on the Origin of Barriers to Internal Rotation about Single Bonds

T. K. Brunck^{1a} and F. Weinhold^{1b}

Contribution from the Biological Sciences Research Center, Shell Development Company, Modesto, California 95352, and the Theoretical Chemistry Institute and Department of Chemistry, University of Wisconsin—Madison, Madison, Wisconsin 53706. Received June 5, 1978

Abstract: An analysis of the forces responsible for internal rotation barriers in ethane-like molecules is carried out in terms of a linear combination of bond orbitals (LCBO) representation of approximate self-consistent field molecular orbitals. The primary contributions to the barrier are found to arise from vicinal interactions between orbitals of bond and antibond type. The preference for staggered conformations in these molecules is traced to the differential stabilizing effects of cis and trans bond-antibond interactions, which in turn can be rationalized from the general shapes of these localized orbitals. Various chemical trends and "effects" of conformational analysis are analyzed from this point of view, and relationships to previous work on the barrier origin are discussed.

I. Introduction

The existence of energy barriers hindering internal rotation about single bonds has been recognized for some 40 years,² but the nature of the forces responsible for these barriers has remained controversial.³ It has sometimes appeared that the barrier results from the interplay of so many factors that no "simple" picture of its origin is possible. Existing theories of the rotation barrier are surveyed in comprehensive review articles.⁴⁻⁸ Here we wish to describe the barrier interactions in terms of a novel method for analyzing delocalized molecular orbitals.

We first review the evidence to indicate that the origin of the barrier is to be found within the Hartree-Fock self-consistent field framework, and even within successive approximations of the self-consistent field molecular-orbital (SCF-MO) theory. A computational method is described which permits the analysis of the delocalized SCF-MOs in terms of localized bond orbitals (BOs), representing localized bonds, antibonds, and lone pairs of the form suggested by elementary valence theory. Such an analysis was in the present case implemented in the INDO (intermediate neglect of differential overlap) approximation of SCF-MO theory. The bond-orbital analysis points to the primary role of the antibonds in the barrier formation, and suggests the importance of the conformational asymmetry of the bond-antibond interactions, which differentially stabilize the staggered and eclipsed geometries. This general picture provides a rationale for several empirical principles of conformational analysis, including "gauche effects", "anomeric effects", and the general dependence on substituent electronegativity. The relationship to previous analyses of the barrier origin is discussed in a concluding section.

II. Rotation Barrier in Hartree-Fock SCF-MO Theory

The Hartree-Fock SCF wave function Φ_{HF} for a closed-shell molecule is the determinantal product of the doubly occupied molecular orbitals (MOs) ϕ_i . The associated Hartree-Fock energy $E_{\text{HF}} = \langle \Phi_{\text{HF}} | \mathcal{H} | \Phi_{\text{HF}} \rangle / \langle \Phi_{\text{HF}} | \Phi_{\text{HF}} \rangle$ for the system with Hamiltonian \mathcal{H} may be written in the form

$$E_{\text{HF}} = 2 \sum_i^{\text{occ}} \epsilon_i - V_{\text{ee}} + V_{\text{nn}} \quad (2.1)$$

where ϵ_i is the orbital energy associated with the i th occupied MO ϕ_i , V_{ee} is the sum of electron-electron repulsions (as represented in terms of the usual Coulomb and exchange integrals J_{ij} , K_{ij})

$$V_{\text{ee}} = \sum_{i,j}^{\text{occ}} (2J_{ij} - K_{ij}) \quad (2.2)$$

and V_{nn} is the sum of nuclear-nuclear repulsions. The subtraction of V_{ee} in (2.1) results, as is well-known, from the implied overcounting of electron-electron repulsions when the orbital energies are summed to approximate the total electronic energy.

Each orbital energy ϵ_i is an eigenvalue of the effective one-electron operator (Fock operator) h_{eff} associated with eigenfunction ϕ_i

$$h_{\text{eff}}\phi_i = \epsilon_i\phi_i \quad (2.3)$$

The Hartree-Fock approximation therefore permits a conceptually useful breakdown of the many-electron interactions into a set of one-electron equations (2.3), but omits the electronic correlation effects which correct for the approximation of self-consistent averaging over the electron-pair repulsions. In practice, eq 2.3 is treated variationally in terms of a finite basis set of atomic orbitals to give approximate SCF-MOs in a linear combination of atomic orbitals (LCAO) form.

In 1963, Pitzer and Lipscomb's⁹ minimal-basis SCF calculation on ethane provided the first numerical evidence that the origin of rotation barriers might be found within the framework of the SCF-MO approximation. There was initial reason to regard the calculated barrier of 3.3 kcal/mol with distrust, for the total energy of each conformer—some 50 000 kcal/mol—depends markedly on such neglected factors as electron correlation, basis-set augmentation, exponent variation, and geometry optimization. Nevertheless, subsequent investigations have shown the ethane barrier to be remarkably insensitive to such refinements.¹⁰ There now seems little doubt that the underlying mechanism of "typical" barriers is to be found within SCF-MO theory.

In the present work we have made use of the well-known INDO¹¹ form of approximate molecular orbital theory. The INDO barrier for ethane itself is compared with the minimal-basis ab initio result in Figure 1a. It can be seen that INDO underestimates the barrier height (2.2 instead of 3.3 kcal/mol), but is otherwise in rough agreement with the ab initio potential, as is also found for other simple threefold barriers. In Figures 1b-g we have compared INDO and ab initio potentials (the latter calculated by Radom et al.¹²) for some molecules expected to represent unusual extremes of barrier behavior. For example, in $\text{NH}_2\text{CH}_2\text{F}$ (Figure 1b), the two outer minima of the usual threefold barrier nearly disappear, while the central (trans) minimum is much deeper; the INDO curve, although too low overall, exhibits these same

Table I. Energy Decomposition of INDO-SCF Rotation Barrier for Some Simple Molecules, Based on Equation 2.4^a

molecule	$2\Sigma_i(\Delta\epsilon_i)$	$-\Delta V_{ee}$	ΔV_{nn}	barrier, kcal/mol
CH ₃ CH ₃	0.0034	-0.0074	0.0076	2.26
CH ₃ NH ₂	0.0014	-0.0042	0.0052	1.51
CH ₃ OH	0.0014	-0.0028	0.0026	0.75

^a All quantities in atomic units unless stated otherwise.

features. Figure 1c illustrates a contrary case (CH₂FOH) in which the central minimum is lost while the two outer (gauche) minima are stabilized; the INDO curve (though again too low) shows these features properly. Figures 1d and 1e for NH₂OH and NH₂OF, respectively, exhibit unusual cases of stable eclipsed conformations; in the NH₂OH case the eclipsed form actually appears as the most stable conformation, while in NH₂OF it forms a secondary minimum, as is also shown in the INDO curves. Finally, in Figures 1f and 1g we show examples of barriers for molecules (NH₂NHF and NHFOH) of lower symmetry. INDO predicts approximately the right stable conformation in the former case (though the overall barrier is again far too low), but gives the wrong conformation in the latter case, where it is difficult to recognize even the qualitative similarities of the barrier profiles. Despite the failures in several cases, it seems fair to conclude that INDO includes at least the qualitative features of the actual barrier interactions, and that an understanding of the INDO barriers is a useful step toward understanding the nature of the barrier forces in higher levels of molecular orbital theory.

Indeed, it is found¹³ that a qualitatively useful picture of barrier potentials persists even in cruder approximations (such as extended Hückel theory), and such methods are widely employed to investigate conformational properties of large molecules.¹⁴ It is remarkable that the small conformational energy differences can appear reasonably constant in spite of rather gross changes in overall energy, orbital energies and orderings, polarities, and other changes associated with these successive levels of approximation. This invariant character is one of the more puzzling aspects which a theory of the barrier origin should seek to explain.

The success of pseudopotential methods¹⁵ (as well as the semiempirical methods mentioned above, which also neglect core electrons) indicates that core electrons do not play a significant role in the barrier mechanism. Furthermore, the available evidence suggests the insensitivity of the ethane barrier to small geometry changes. However, two such factors that are individually unimportant can interact to give an apparent (but spurious) dependence on conformation. For example, when the ethane geometry is carefully optimized at each torsional angle, the core energies (which depend strongly on C-C bond length) show a dependence on the torsional angle which is about three times as large as the total rotation barrier,¹⁶ though the barrier itself is scarcely affected. For this reason we consider it preferable to keep the molecular geometry fixed (except for the torsional angle), and we have followed the work of Pople and Gordon¹⁷ in adopting idealized bond lengths and angles for all the molecules considered.

Each component of the total energy expression (2.1) may be examined for its dependence on the dihedral angle α of internal rotation:

$$E_{\text{HF}}(\alpha), \epsilon_i(\alpha), V_{ee}(\alpha), V_{nn}(\alpha)$$

In particular, the total barrier height $E_{\text{HF}} = E_{\text{HF}}(\text{eclipsed}) - E_{\text{HF}}(\text{staggered})$ may be decomposed in the usual way¹⁸ into separate contributions ΔV_{nn} , ΔV_{ee} , and $\Delta\epsilon_i$ in the form

$$\Delta E_{\text{HF}} = 2 \sum_i^{\text{occ}} \Delta\epsilon_i - \Delta V_{ee} + \Delta V_{nn} \quad (2.4)$$

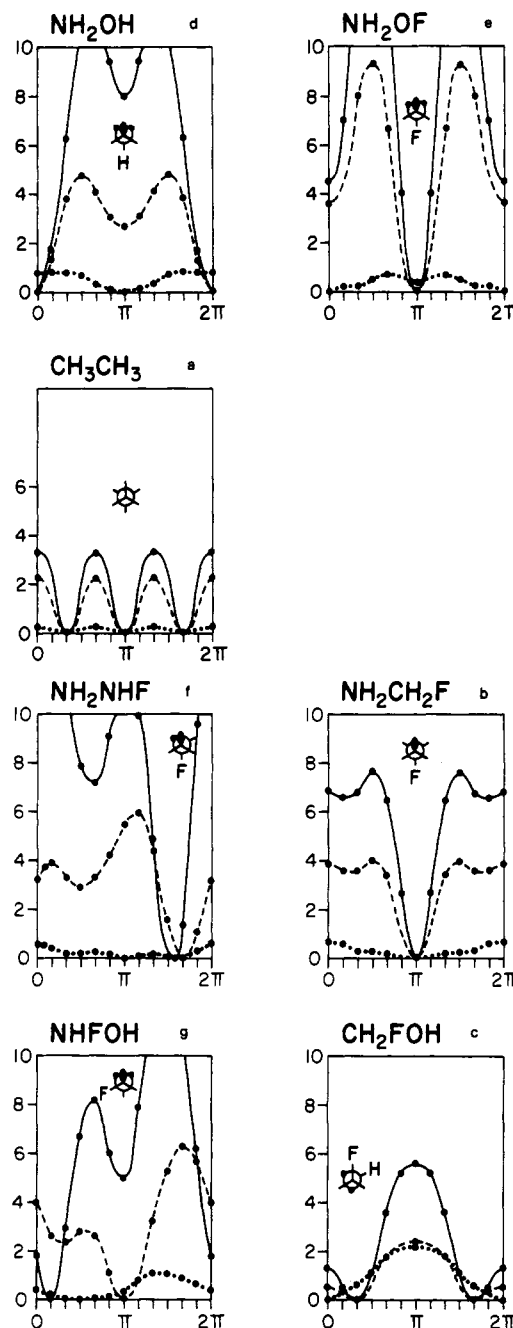


Figure 1. Comparison of ab initio (solid line —) and INDO (dashed line ---) SCF-MO barrier potentials for some ethane-like molecules: (a) CH₃CH₃, (b) NH₂CH₂F, (c) CH₂FOH, (d) NH₂OH, (e) NH₂OF, (f) NH₂NHF, (g) NHFOH. The ordinates (potential energy) and abscissas (torsional angle) are each on the scale of 0–10 kcal/mol and 0–360°, respectively. Also shown for each molecule is the “σ only” INDO barrier (dotted line ····) which results when antibonds are omitted from the basis set; see section IV A.

as shown for some simple barriers (in the INDO approximation) in Table I. The entries show that most of the barrier arises from the conformational dependence of the orbital energies, rather than from the V_{ee} and V_{nn} terms, which approximately cancel. (This near cancellation of ΔV_{ee} and ΔV_{nn} is of course implied by the partial success of extended Hückel and related methods which employ only the orbital energies to calculate the total energy.) The initial objective is therefore to understand the conformational dependence of the SCF orbital energies ϵ_i . For this purpose we describe a method of analyzing these orbital energies in terms of the interactions of localized bonds, antibonds, and lone pairs in the following section.

Table II. Diagonal INDO Matrix Elements $H_{\sigma\sigma}$ (au) for CH Bonds in Various Molecules, Illustrating the Approximate Transferability of Bond Orbital Energies

molecule	CH bond energy	molecule	CH bond energy
CH ₄	-0.861	CH ₃ NH ₂	-0.865
CH ₃ CH ₃	-0.862	CH ₃ OH	-0.877
	-0.864		-0.879
CH ₃ CH ₂ CH ₃	-0.865		-0.881
	-0.866	CH ₂ FCH ₃	-0.884
CH ₂ F ₂	-0.942		-0.896

III. LCBO-MO Theory

Conceptual analysis of the delocalized SCF-MOs is facilitated by writing them in a linear combination of bond orbitals (LCBO) form. The LCBO-MO approach has been previously employed to discuss "through-bonds" interactions¹⁹ and the phase-extended principles of maximum overlap which are useful in interpreting such interactions.²⁰ Detailed computational aspects of the LCBO-MO method are described in a forthcoming paper,²¹ but we summarize those features which are pertinent to the present discussion.

The SCF-MOs are usually expressed as linear combinations of atomic orbitals (AOs) χ_μ

$$\phi_i = \sum_\mu a_{i\mu} \chi_\mu \quad (3.1)$$

which we take to be orthonormal, $\langle \chi_\mu | \chi_\nu \rangle = \delta_{\mu\nu}$. The coefficients $a_{i\mu}$ are obtained from the eigenvectors \mathbf{a}_i of the SCF eigenvalue equation

$$\tilde{\mathbf{H}}\mathbf{a}_i = \epsilon_i \mathbf{a}_i \quad (3.2a)$$

with matrix elements

$$\tilde{H}_{\mu\nu} = \langle \chi_\mu | h_{\text{eff}} | \chi_\nu \rangle \quad (3.2b)$$

Because the customary AOs are neither hybridized nor oriented in a manner corresponding to the local bonding requirements, the matrix elements $\tilde{H}_{\mu\nu}$ are not readily transferable from one bonding environment to another, nor do they exhibit a simple pattern. For this reason the LCAO representation (3.1) is often inconvenient for conceptual purposes.

A more suitable basis set for describing σ electrons is obtained by first hybridizing the primitive χ_μ 's on each atom, and orienting these hybrids toward the neighboring atoms to be bonded. The directed hybrid orbitals h_μ are then formed into appropriate in-phase and out of phase linear combinations

$$\sigma_{\mu\nu} = 2^{-1/2}(h_\mu + h_\nu) \quad (3.3a)$$

$$\sigma^*_{\mu\nu} = 2^{-1/2}(h_\mu - h_\nu) \quad (3.3b)$$

of bond and antibond type, or are left as lone-pair orbitals

$$n_\mu = h_\mu \quad (3.3c)$$

in the manner suggested by elementary valence theory. We denote these bond orbitals (BOs)—whether of bond (σ), antibond (σ^*), or lone-pair (n) type—by the symbol Ω_i .

$$\Omega_i = \begin{cases} \sigma, \text{ bond} \\ \sigma^*, \text{ antibond} \\ n, \text{ lone pair} \end{cases} \quad (3.4)$$

The AOs χ_μ and BOs Ω_i are connected by a unitary transformation \mathbf{U} :

$$\{\chi_\mu\} \xrightarrow{\mathbf{U}} \{\Omega_i\} \quad (3.5a)$$

of the form

$$\Omega_i = \sum_\mu U_{i\mu} \chi_\mu \quad (3.5b)$$

The transformed basis set $\{\Omega_i\}$ leads to the transformed eigenvalue equation

$$\mathbf{H}\mathbf{b}_i = \epsilon_i \mathbf{b}_i \quad (3.6a)$$

with matrix elements

$$H_{ij} = \langle \Omega_i | h_{\text{eff}} | \Omega_j \rangle \quad (3.6b)$$

The transformed eigenvalue equation (3.6) leads to the same set of orbital energies and molecular orbitals as before, but the latter are now expressed in LCBO form:

$$\phi_i = \sum_j b_{ij} \Omega_j \quad (3.7)$$

where the LCBO coefficients b_{ij} are related to those of the LCAO expansion (3.1) by

$$b_{ij} = \sum_\mu U^*_{j\mu} a_{i\mu} \quad (3.8)$$

In the BO basis (3.6b), the diagonal elements H_{ii} of the effective Hamiltonian operator represent the electronic energies of localized bonds, antibonds, or lone pairs, and are found to be reasonably transferable from one molecule to another, as elementary valence theory would suggest. Table II exhibits this transferability for a C-H bond orbital in various small molecules (as calculated in the INDO-SCF-MO approximation), showing the variation to be of the order of a few percent. The off-diagonal H_{ij} 's are small (typically an order of magnitude less than corresponding H_{ii} 's), and represent the weak interactions of the localized bond orbitals which give rise to the delocalization of the final molecular orbital. In the LCBO-MO expansion (3.7), the delocalized MOs ϕ_i are therefore expressed directly as superpositions of the localized bonds, antibonds, and lone pairs which are the "unperturbed" units of the σ electronic structure.

One should distinguish between the foregoing LCBO theory of the "canonical" molecular orbitals (CMOs) and the theory of "localized" molecular orbitals (LMOs) as developed by Edmiston and Ruedenberg, Boys, and others.²² The LMOs are obtained by mixing together delocalized CMOs

$$\text{LMO} = \sum (\text{coef}) \cdot (\text{CMO}) \quad (3.9a)$$

to obtain more localized entities, whereas the LCBO expansion (3.7) is of the form

$$\text{CMO} = \sum (\text{coef}) \cdot (\text{BO}) \quad (3.9b)$$

showing that CMOs are decomposed into (rather than mixed together to form) the localized functions. The LMOs are less useful for the present purposes; although any nonsingular linear transformation of CMOs would lead to the same wave function and total energy, *only* the CMOs themselves have the direct spectroscopic significance associated with Koopmans' theorem and with their role as eigenfunctions of the effective Hamiltonian operator of the system.²³ However, the LCBO analysis allows one to make contact with the localized entities which were sought in the LMO transformation. In effect, the LCBO-MO technique brings a set of valence-bond-like concepts into the analysis of delocalized molecular orbitals.

IV. LCBO Analysis of the Ethane Barrier in INDO-SCF-MO Theory

A. Bond-Antibond Partitioning of the Fock Matrix. Using the INDO-SCF-MO method, we investigated the rotation barrier of ethane in the LCBO framework. The calculations were made in the rigid-rotor approximation, with idealized

Table III. Geometry Dependence of INDO-SCF Rotation Barrier for Ethane

C-C bond length, Å	C-H bond length, Å	$2\Sigma_i(\Delta\epsilon_i)$, au	rotation barrier, au (kcal/mol)	% change
1.536	1.093	0.0034	0.0036 (2.26)	
1.536	1.043	0.0032	0.0033 (2.07)	-8
1.536	1.143	0.0036	0.0038 (2.38)	+5
1.486	1.093	0.0038	0.0043 (2.70)	+19
1.586	1.093	0.0030	0.0030 (1.86)	-18

geometries (C-C = 1.536 Å, C-H = 1.093 Å, tetrahedral angles). The INDO barrier is then 2.26 kcal/mol, rather less than the experimental value of about 2.9 kcal/mol,²⁴ but within the general range of values calculated by various ab initio and semiempirical SCF procedures. The insensitivity to small geometry changes is indicated in Table III, where the INDO barrier is seen to change by less than about 20% under 0.050-Å distortions of C-C and C-H bond lengths.

In the LCBO framework, the basis set divides naturally into bonding (σ) and antibonding (σ^*) components, thus permitting a partitioning of the effective Hamiltonian matrix **H** into bonding and antibonding blocks:

$$\mathbf{H} = \begin{bmatrix} \mathbf{H}_{\sigma\sigma} & \mathbf{H}_{\sigma\sigma^*} \\ \mathbf{H}_{\sigma^*\sigma} & \mathbf{H}_{\sigma^*\sigma^*} \end{bmatrix} \begin{matrix} \sigma \\ \sigma^* \end{matrix} \quad (4.1)$$

Inclusion of the full ($\sigma + \sigma^*$) BO basis simply recovers the "exact" SCF result, since it corresponds to a unitary transformation of the original AO basis. But the effects of individual bonds and antibonds may now be examined by truncating the matrix in various ways. For example, in the interpretation of through-bond effects,¹⁹ it was found that antibonding BOs play no significant role in the general shape or energy of the occupied MOs, and that truncation of the BO basis to the bonding orbitals alone

$$\mathbf{H}_{\sigma\sigma}\mathbf{b}_i^{(\sigma)} = \epsilon_i^{(\sigma)}\mathbf{b}_i^{(\sigma)} \quad (4.2a)$$

gives a qualitatively correct picture of these interactions. In this approximation the molecular orbitals take the form

$$\phi_i^{(\sigma)} = \sum_j b_{ij}^{(\sigma)} \Omega_j^{(\sigma)} \quad (4.2b)$$

where, as indicated, the index j runs only over Ω_j 's of bonding type.

Although the antibonds superficially have little effect on the occupied molecular orbitals, they nevertheless make significant contributions to the rotation barrier. This can be seen most readily in Figures 1a-g, where we have also plotted (as the dotted curves marked " σ only") the barriers which result when antibonds are omitted from the basis set. It is evident that these latter curves bear little resemblance to the full SCF barrier potentials, and that the omitted bond-antibond (and, to a lesser extent, antibond-antibond) interaction terms must constitute the dominant contribution to the INDO rotation barrier. The same conclusion can be drawn from the entries of Table IV, which shows the energy contributions of eq 2.1 as calculated with and without the antibonds. We have included the results for an "unpolarized" basis (3.3) as well as for a "polarized" basis:

$$\sigma_{\mu\nu}^{(\text{pol})} = \lambda h_\mu + (1 - \lambda^2)^{1/2} h_\nu \quad (4.3a)$$

$$\sigma_{\mu\nu}^{*(\text{pol})} = (1 - \lambda^2)^{1/2} h_\mu - \lambda h_\nu \quad (4.3b)$$

in which the parameter $\lambda = 0.659$ is chosen to reflect the electronegativity differences in the C-H bond (with $\mu = \text{C}$, $\nu = \text{H}$). In general, such a parameter can be adjusted to give the

+0.0031	+0.0031	$e_g (e'')$	+0.0020	+0.0020
-0.0003		$a_{1g} (a_1')$	0.0000	
-0.0030	-0.0030	$e_u (e')$	-0.0014	-0.0014
+0.0009		$a_{2u} (a_2'')$	+0.0007	
-0.0005		$a_{1g} (a_1')$	-0.0002	
POLARIZED σ BASIS			FULL $\sigma + \sigma^*$ BASIS	

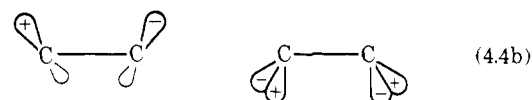
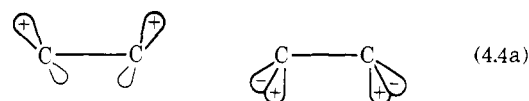
Figure 2. General pattern of INDO valence orbital energy levels and their barrier contributions $\Delta\epsilon_i$ for ethane, as calculated with omission (left) and inclusion (right) of antibonds. Each orbital is labeled with the symmetry designation of the D_{3d} (staggered) and D_{3h} (eclipsed) point groups, with all energy contributions expressed in atomic units.**Table IV.** INDO Rotation Barrier and Energy Components for Ethane, Calculated with Various Basis Sets (See Text)^a

basis set	$2\Sigma_i(\Delta\epsilon_i)$	$-\Delta V_{ee}$	ΔV_{nn}	barrier, kcal/mol
$\sigma + \sigma^*$ (full)	0.0034	-0.0074	0.0076	2.26
polarized σ	0.0006	-0.0078	0.0076	0.25
unpolarized σ	0.0002	-0.0074	0.0076	0.25

^a All quantities in atomic units unless stated otherwise.

unique set of bonds and antibonds for which the contribution of antibonds to the occupied MOs is a minimum.²¹ As can be seen from Table IV, the terms are relatively insensitive to this polarization, but the effect of omitting the antibonds is in each case to reduce the barrier to an unphysically small value.

B. Bond-Bond Interactions. A general picture of the origin of the rotation barrier can now be constructed in terms of the LCBO decomposition into bond-bond and bond-antibond contributions (the antibond-antibond terms being of lesser importance). Let us first examine the structure of the occupied MOs in terms of the $\Omega_j^{(\sigma)}$ bond-type BOs (the σ basis) alone. Figure 2 shows the relative energies and degeneracies of the seven occupied valence MOs of ethane, as calculated in the polarized σ basis and full ($\sigma + \sigma^*$) basis. With each orbital is given its contribution $\Delta\epsilon_i$ to the rotation barrier. Figure 2 indicates that the two pairs of degenerate e orbitals are most sensitive to the dihedral rotation angle α , as has previously been noted.²⁵ That this should be so can be seen from the qualitative forms of these MOs in terms of their constituent BOs; the lower pair is predominantly the *in*-phase combination of vicinal C-H bonds (as shown (4.4a) in the eclipsed geometry) while the upper pair is the corresponding out of phase combination (4.4b). The orbitals (4.4a) will evidently favor the eclipsed



conformation as shown, which gives additional overlap reminiscent of the π overlap in ethylene. However, the other pair (4.4b) should prefer the staggered conformation by nearly the same energy difference, since the eclipsed conformation brings the C-H bond orbitals into a more antibonding (destabilizing) arrangement. Since these orbitals are fully occupied, the net result is that upper and lower e levels make nearly canceling contributions to the rotation barrier when only the bond-bond interactions are considered.

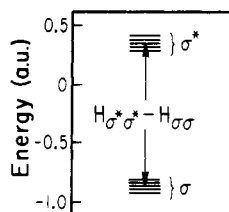


Figure 3. General distribution of bond and antibond orbital energies in hydrocarbons, illustrating the large energy separation of $H_{\sigma\sigma^*}$ and $H_{\sigma\sigma}$ elements.

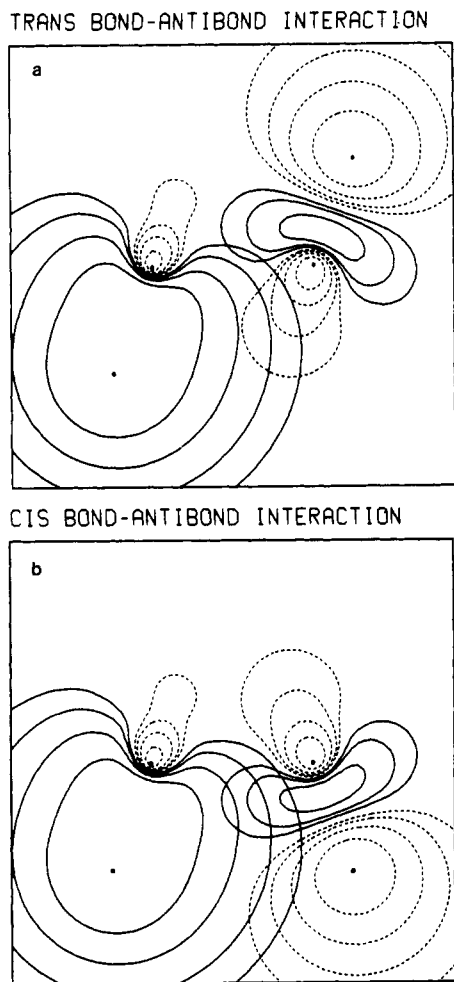
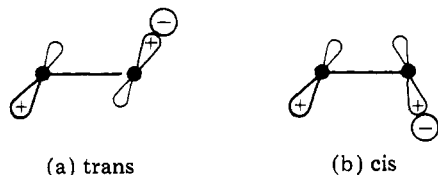


Figure 4. Interaction of vicinal CH bond and antibond orbitals in ethane for the trans (a) and cis (b) orientation. Solid (dashed) lines represent



orbital amplitude contours of positive (negative) phase, each contour (to the outermost at 0.2) corresponding to half the amplitude of the preceding one. Dots indicate the positions of the nuclei.

[That it is primarily the degenerate e levels which are sensitive to torsional angle can be understood²⁵ from the fact that the nondegenerate levels necessarily possess the full threefold symmetry at each end of the molecule, so that the gain or loss of overlap is less than in the asymmetric orbitals (4.4).]

C. Bond-Antibond Interactions. To see how this picture is altered as the antibonds are brought into the basis set, one may use simple second-order perturbation theory to estimate the energy lowering $\delta\epsilon_\sigma$ of a bond orbital σ due to its interaction

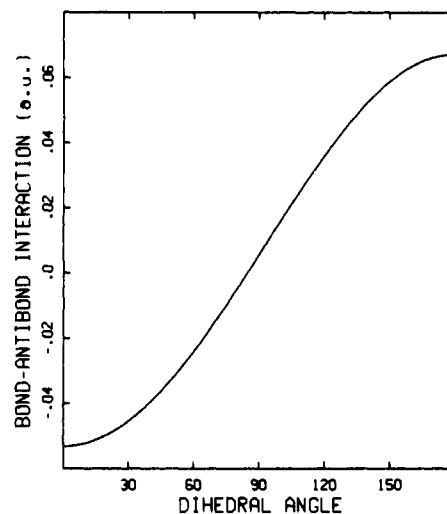


Figure 5. Calculated bond-antibond interaction matrix element $H_{\sigma\sigma^*}$ for vicinal CH bond and antibond in ethane (in the INDO-SCF-MO approximation), shown as a function of torsional angle (0° = cis, 180° = trans).

with an antibonding level σ^* :

$$\delta\epsilon_\sigma \approx \frac{H_{\sigma\sigma^*}^2}{H_{\sigma\sigma^*} - H_{\sigma\sigma}} \quad (4.5)$$

This estimate should be reasonably adequate in the present case, since the off-diagonal bond-antibond interaction elements $H_{\sigma\sigma^*}$ are indeed small relative to the diagonal elements, and the bonding and antibonding manifolds are well separated in energy as depicted in Figure 3, so that the energy denominator in eq 4.5 is large (of order unity). Thus, the formal requirements of low-order perturbation theory are well satisfied.

As Figure 3 suggests, the energy denominators in (4.5) are roughly equal for any pair of orbitals chosen from the σ and σ^* C-H manifolds, so that little significant stabilization can be expected from this source. However, the vicinal bond-antibond interaction matrix elements $H_{\sigma\sigma^*}$ of the numerator can depend *markedly* on conformation, and thus give rise to significant differential stabilization of the staggered and eclipsed geometries.

The conformational asymmetry of the bond-antibond interactions is pictured in Figure 4, where we show a bond and an antibond orbital as oriented in a mutually trans or cis arrangement in Figures 4a and 4b, respectively. It is clear that these interactions must be different. Simple considerations of overlap suggest (correctly) that *the trans bond-antibond interaction is stronger (more stabilizing) than is the cis interaction*.²⁶ In ethane, the INDO numerical values of the numerators in (4.5) are, in au

$$H_{\sigma\sigma^*}^2(\text{trans}) = 0.0045, H_{\sigma\sigma^*}^2(\text{cis}) = 0.0028 \quad (4.6)$$

suggesting that a trans $\sigma\sigma^*$ interaction will be about 60% more effective in lowering the orbital energy than will a corresponding cis interaction. While the differences are small in an absolute sense, they are precisely of the order of barrier energies, and they could be expected to appear in a consistent way in ethane-like molecules. The full torsional dependence of an INDO bond-antibond interaction element $H_{\sigma\sigma^*}$ for ethane is shown in Figure 5. One can also see from this figure that the remaining $\sigma\sigma^*$ interactions, at 60° in the staggered conformation or 120° in the eclipsed, are smaller and more nearly canceling than are the cis and trans interactions on which we concentrate.

It can then be understood why the staggered conformation is energetically favored by the bond-antibond interactions,

since only in this form are C-H bonds and antibonds arranged in the favorable trans orientation. We have attempted to crudely represent the effect of antibonds in a kind of "correlation diagram" in Figure 6, where the orbital energies of the degenerate e orbitals in both staggered (S) and eclipsed (E) geometries are plotted against the extent of "antibond participation". As antibonds are brought into interaction with bonds (passing to the right of the diagram), the S levels are more stabilized by the trans $\sigma\sigma^*$ interaction; this tends to increase the preference of the upper orbitals for the S conformation while diminishing that of the lower orbitals for the E form, thus leading to net stabilization of the staggered conformer. Such considerations draw attention not to any "repulsions" leading to a "barrier", but rather to the stabilizing interactions leading to energy "wells" or "valleys" at those favorable dihedral angles where the number of trans bond-antibond interactions is maximized.

Such arguments also suggest why the rotation barrier should appear with consistency in many levels of molecular orbital theory. In any LCAO calculation having at least a *minimal* basis of AOs, the basis set implicitly contains both the important bonds and antibonds. As long as these orbitals have *approximately* the correct shape (as shown in Figure 4), and as long as the energy denominator of (4.5) (i.e., the gross separation of bonding and antibonding manifolds) is roughly correct, one could expect a barrier contribution of roughly the correct magnitude. Such qualitative features of the orbital interactions should persist even in crude levels of molecular orbital theory.

V. General Characteristics of Bond-Antibond Interactions. Gauche Effects, Anomeric Effects, and Related Aspects of Conformational Analysis

A. Bond-Antibond Interactions. A useful energy decomposition scheme should make it possible to rationalize and predict various chemical trends in barrier potentials. The LCBO theory leads (when bond-bond interaction terms are small) to a decomposition of these potentials in terms of an approximately additive set of bond-antibond interactions

$$\Delta E \approx \sum_{\text{vicinal pairs, } \epsilon_{\sigma\sigma^*} - \epsilon_{\sigma}} \frac{H_{\sigma\sigma^*}^2}{\epsilon_{\sigma\sigma^*} - \epsilon_{\sigma}} [+ \Delta E_{\text{bond-bond}}] \quad (5.1)$$

each of which depends in a definite way on the chemical substituents. In this section we wish to draw out some of the chemical trends and rules of conformation preference that are suggested by this picture.

It is a crude but useful first approximation to neglect the energy denominators of (5.1), since variations in ϵ_{σ} or $\epsilon_{\sigma\sigma^*}$ are usually small compared to their overall separation, and these denominators therefore have only a secondary influence on conformational preferences. It is also useful to recall the crude proportionality of Hamiltonian matrix elements $H_{\sigma\sigma^*}$ to the overlap of the (nonorthogonalized) orbitals

$$H_{\sigma\sigma^*} \propto S_{\sigma\sigma^*}(\text{nonorthogonal})$$

which allows the strengths of the bond-antibond interactions to be crudely discussed in terms of the general shapes of these orbitals.

Consider first the case of a monosubstituted ethane $\text{CH}_3\text{CH}_2\text{X}$. Relative to ethane itself, two of the six vicinal $\sigma_{\text{CH}}-\sigma_{\text{CH}}^*$ interactions are replaced by one each of $\sigma_{\text{CH}}-\sigma_{\text{CX}}^*$ and $\sigma_{\text{CX}}-\sigma_{\text{CH}}^*$ type. If the substituent bond polarity is C^+X^- , one expects the bond orbital σ_{CX} to be primarily concentrated on the ligand X, while the antibond σ_{CX}^* is correspondingly concentrated on the axial C. The $\sigma_{\text{CX}}-\sigma_{\text{CH}}^*$ interactions should therefore be somewhat weaker (less stabilizing) and the $\sigma_{\text{CH}}-\sigma_{\text{CX}}^*$ interactions somewhat stronger (more stabilizing) than ordinary $\sigma_{\text{CH}}-\sigma_{\text{CH}}^*$ interactions. Conversely, if the axial C is replaced by some atom M to give a bond of polarity

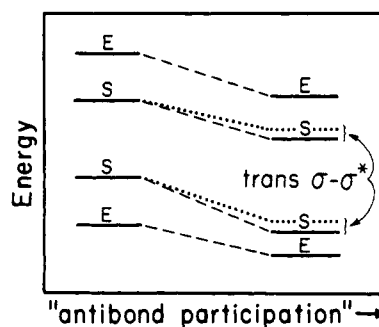


Figure 6. Schematic "correlation diagram" for degenerate e orbitals of ethane, showing preferential stabilization of staggered conformation with increased "antibond participation". See text.

Table V. Typical Matrix Elements $H_{\sigma\sigma^*}^2$ (au) for Various Types of σ (Row) and σ^* (Column) Orbitals^a

bond	antibond		
	σ_{CX}^*	σ_{CH}^*	σ_{MH}^*
n	0.0112	0.0071	0.0049
	0.0111	0.0046	0.0021
σ_{MH}	0.0073	0.0050	0.0034
	0.0087	0.0031	0.0011
σ_{CH}	0.0067	0.0045	0.0034
	0.0080	0.0028	0.0012
σ_{CX}	0.0042	0.0030	0.0021
	0.0050	0.0014	0.0004

^a The upper and lower entry represent the trans and cis value, respectively. These orbitals are chosen from various molecules, with X = fluorine, M = nitrogen, n = nitrogen lone pair. Note that particular matrix elements will have slightly different values in different molecular environments.

M^-H^+ , one could expect $\sigma_{\text{MH}}-\sigma_{\text{CH}}^*$ and $\sigma_{\text{CH}}-\sigma_{\text{MH}}^*$ to be more and less stabilizing, respectively, than $\sigma_{\text{CH}}-\sigma_{\text{CH}}^*$. By the same reasoning, $\sigma_{\text{MH}}-\sigma_{\text{CX}}^*$ should be still more stabilizing, and $\sigma_{\text{CX}}-\sigma_{\text{MH}}^*$ still less stabilizing, than $\sigma_{\text{CH}}-\sigma_{\text{CH}}^*$, and the most favorable interaction would occur in the case of a lone-pair orbital n interacting with the σ_{CX}^* antibond. One can say in general that the bond-antibond stabilization energy should be greater as the *bond* is chosen from

$$n > \sigma_{\text{MH}} > \sigma_{\text{CH}} > \sigma_{\text{CX}} \quad (5.2)$$

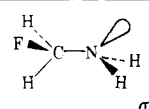
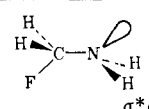
and as the *antibond* is chosen from

$$\sigma_{\text{CX}}^* > \sigma_{\text{CH}}^* > \sigma_{\text{MH}}^* \quad (5.3)$$

These trends are numerically illustrated in Table V with INDO Hamiltonian matrix elements for the various interaction types, with X = fluorine and M = nitrogen. Note that interactions involving CH (or MH) bonds are stronger than might be expected from polarity considerations alone, owing to the shorter H covalent radius. It is evident from Table V that the bond-antibond interactions vary systematically in the manner suggested by (5.2) and (5.3). It is also apparent that the relative differences can be quite large; for example, the trans $n-\sigma_{\text{CF}}^*$ interaction is approximately five times larger than that for $\sigma_{\text{CF}}-\sigma_{\text{NH}}^*$, and the corresponding cis differences are still larger. While one should not attribute great quantitative significance to the numerical values of these INDO matrix elements, the overall trends are chemically reasonable and numerically quite pronounced. Thus, the overall picture should not be greatly altered in more realistic levels of molecular orbital theory.

Table V indicates that the relative strength of cis and trans interactions depends most sensitively on the choice of antibond. This would also be suggested by the orbital diagrams of Figure

Table VI. Bond-Antibond Interactions in Conformers of CH_2FNH_2 (as Estimated from the Entries of Table V), Showing the Stabilization of the Trans Form (b)^a

			
	$\sigma\sigma^*$	$\sigma^*\sigma$	
n-CH	0.0071		0.0071
NH-CF	0.0073	0.0021	0.0094
NH-CH	0.0050	0.0034	0.0084
		total	0.0249
(a) gauche			
			
	$\sigma\sigma^*$	$\sigma^*\sigma$	
n-CF	0.0112		0.0112
NH-CH	0.0050	0.0034	0.0084
NH-CH	0.0050	0.0034	0.0084
		total	0.0280
(b) trans			

^a All entries in atomic units.

4, since the position of the antibonding nodal surface will be most important in controlling the amount of "cancellation" which occurs in the cis orientation. As this nodal surface recedes toward the ligand with increasing electronegativity of X, the cis interaction should gain faster than does the trans, and may eventually lead to a net eclipsing force. Thus, in fluoroethane in the INDO approximation, the $\sigma_{\text{CH}}-\sigma^*_{\text{CF}}$ matrix element slightly favors the eclipsed rotamer (though the one $\sigma_{\text{CF}}-\sigma^*_{\text{CH}}$ and four $\sigma_{\text{CH}}-\sigma^*_{\text{CH}}$ interactions continue to favor the staggered form).

It is evident that significant change in the barrier height results when the number of vicinal bond-antibond interactions is reduced. This occurs when lone pairs replace chemical bonds at either end of the torsional axis, for in this case there is no corresponding antibond, and at least one of the trans $\sigma\sigma^*$ interactions is lost. While this loss is partially compensated by the greater strength of the remaining $\sigma\sigma^*$ interactions when " σ " is a lone pair (cf. Table V), one can expect that the barrier is reduced with increasing numbers of lone pairs, as in the series CH_3CH_3 , CH_3NH_2 , CH_3OH . In cases where one chemical bond is replaced by another (rather than by a lone pair), the total number of bond-antibond interactions is conserved, and the effect on the barrier may be surprisingly small (as in fluoroethane, where INDO predicts a barrier change of only about 0.2 kcal/mol). However, proper discussion of relative barrier heights in dissimilar molecules would necessarily require examination of electrostatic, steric, and other factors beyond those considered here, and so will not be further pursued.

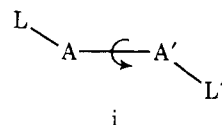
B. Conformational Isomerism. Since the staggered form will be favored over the eclipsed form in the great majority of ethane-like molecules, it is perhaps more interesting to inquire which of several possible staggered conformations will be preferred, i.e., to determine the relative stabilities of conformational isomers. Estimates of these stabilities can be based on the trans $\sigma\sigma^*$ matrix elements of Table V, which should dominate the conformational preference when gross steric and electrostatic effects (of the type described by the bond-bond interactions) are not too large.

Consider, for example, the molecule fluoromethylamine (CH_2FNH_2), which can exist in either the gauche or trans isomeric forms²⁷ shown in Table VI. The six vicinal bond-antibond interactions for each conformer, as taken from Table V, are shown in this table. Simple addition of these matrix elements [cf. (5.1)] suggests that the bond-antibond interactions must stabilize the trans form (0.028) more than the gauche form (0.025), as the full INDO calculation confirms (see Figure 1b). Comparing the entries of Table VI in more detail, one sees that a CH-NH ($\sigma_{\text{CH}}-\sigma^*_{\text{NH}}$ and $\sigma_{\text{NH}}-\sigma^*_{\text{CH}}$) pair is common to both conformers, and can be ignored. Of the remaining entries, the n- σ^*_{CF} term (which exceeds the corresponding n- σ^*_{CH} of the gauche conformer by 0.004) evidently dominates the comparison. The lone-pair elements of Table V are so much larger than other interactions that one can generally anticipate that

(a) *Because of their strong interactions with vicinal antibonds, lone pairs will often dominate the conformational preference.*

In the present case, the lone pair naturally orients trans to the CF bond (with which it has the largest interaction of Table V) rather than to one of the CH bonds.

It is convenient to let A ("axial") and L ("ligand") denote atoms of a general A-L bond in which A lies on the rotor axis, as in i. We describe the A-L pair as "A-polar" if the bonding

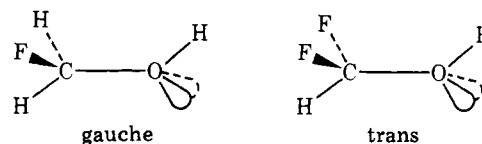


electron density is polarized predominantly toward the axial atom (i.e., if A is more electronegative than L), and "L-polar" if predominantly polarized toward the ligand (i.e., if L is more electronegative than A). This implies that an A-polar antibond is predominantly polarized toward the ligand L, while L-polar antibonds are correspondingly polarized toward the axis. One can then summarize (5.2), (5.3), and the trends of Table V as follows.

(b) *The strongest (vicinal) bond-antibond interactions occur between A-polar bonds and L-polar antibonds.*

In this context, a lone pair is an extreme type of A-polar "bond", for which there is no corresponding antibond. Evidently a lone pair will prefer to orient trans to the *most* L-polar group available at the other end of the rotor axis, in order to take best advantage of the bond-antibond interactions. This accounts simply for the preferred conformation (Table VIb) of fluoromethylamine.


A similar preference could be anticipated in molecules like CHF_2NH_2 , CH_2FOH , CHF_2OH , and so forth, where lone pairs again may choose to lie trans to either a highly L-polar CF bond or to a largely unpolarized CH bond, and where the former choice always leads to better bond-antibond stabilization. This is shown in Table VII for the two conformers of CHF_2NH_2 , showing the expected stabilization of the gauche form (Table VIIb). In a similar way, one expects the preferred conformations of CH_2FOH and CHF_2OH to be the gauche




and trans forms, respectively, the preference being particularly strong in the latter case, where there are two trans n- σ^*_{CF} interactions. In each case, these expectations are confirmed by a full INDO calculation. More generally, one may anticipate that

(c) *Preferred conformations will tend to maximize the (A-polar)-(L-polar) differences across trans arrangements of vicinal groups (particularly those involving lone pairs).*

Table VII. Bond-Antibond Interactions in Conformers of CF_2HNH_2 (as Estimated from the Entries of Table V), Showing the Stabilization of the Gauche Form (b)^a



(a) trans



(b) gauche

	$\sigma\sigma^*$	$\sigma^*\sigma$		$\sigma\sigma^*$	$\sigma^*\sigma$	
n-CH	0.0071		0.0071	n-CF	0.0112	0.0112
NH-CF	0.0073	0.0021	0.0094	NH-CF	0.0073	0.0021
NH-CF	0.0073	0.0021	0.0094	NH-CH	0.0050	0.0034
	total		0.0259		total	

(a) trans
(b) gauche

^a All entries in atomic units.**Table VIII.** Bond-Antibond Interactions in Conformers of NH_2NH_2 (as Estimated from the Entries of Table V), Showing the Stabilization of the Gauche Form (b)^a

Journal of Molecular Structure

Diagram (a) shows the trans conformation of hydrazine (NH₂NH₂). The two nitrogen atoms are connected by a single bond. Each nitrogen atom is bonded to two hydrogen atoms. The lone pairs on the nitrogen atoms are shown as lobes, one pointing up and one pointing down, in a trans arrangement relative to the N-N bond.

	$\sigma\sigma^*$	$\sigma^*\sigma$	
n-n			
NH-NH	0.0034	0.0034	0.0068
NH-NH	0.0034	0.0034	0.0068
	total		0.0136

(a) trans

Diagram (b) shows the gauche conformation of hydrazine (NH₂NH₂). The two nitrogen atoms are connected by a single bond. Each nitrogen atom is bonded to two hydrogen atoms. The lone pairs on the nitrogen atoms are shown as lobes, one pointing up and one pointing down, in a gauche arrangement relative to the N-N bond.

	$\sigma\sigma^*$	$\sigma^*\sigma$	
n-NH	0.0049		0.0049
n-NH	0.0049		0.0049
NH-NH	0.0034	0.0034	0.0068
	total		0.0166

(b) gauche

^a All entries in atomic units.

Similar reasoning must apply in the case of vicinal lone pairs, as in hydrazine (Table VIII). There must be a strong electronic tendency to orient each lone pair trans to an N-H bond rather than to the other lone pair (where the trans $\sigma\sigma^*$ interactions would be lost entirely). Thus, as Table VIII indicates, vicinal lone pairs should orient preferentially in a gauche conformation, in order that each may lie trans to an N-H bond. More generally

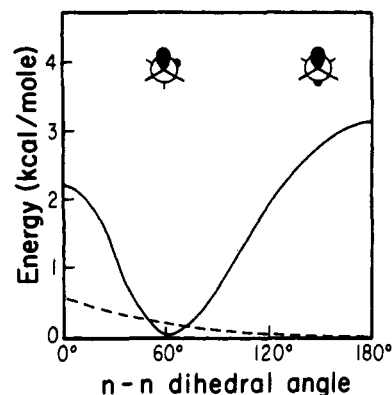
(d) *Vicinal lone pairs each tend to orient trans to the most L-polar group available, and hence gauche to one another.*

Figure 7 shows the full INDO barrier potential for the case of hydrazine, illustrating the expected stabilizations of the gauche conformer. In this case, the bond-bond interactions alone (dashed curve) would favor the trans isomer, as simple steric considerations might suggest. However, inclusion of the bond-antibond interactions completely alters the barrier profile to give the result expected from the qualitative considerations above. Note that the gauche preference does not result from any specific "repulsion" of lone pairs, but is a consequence of their stabilizing interactions with vicinal antibonds.

By a similar line of reasoning one can expect that an L-polar C-X bond should prefer to lie trans to a C-H bond (or other A-polar group) rather than to another L-polar bond, since the $\sigma_{\text{CH}}-\sigma^*_{\text{CX}}$ interaction is then used to best advantage. That is, the C-X antibond can dominate the conformational choice, just as a lone pair can dominate as a "bond" orbital. A corollary is that molecules with vicinal L-polar bonds, such as 1,2-difluoroethane, can have an electronic preference for gauche conformations, contrary to what would naively be expected on the basis of dipolar interactions.

(e) *Vicinal L-polar bonds each tend to orient trans to the most A-polar group available, and hence gauche to one another.*

Of course, the dipolar interactions, which enter primarily through the bond-bond interactions, will work to oppose this bond-antibond effect (for example, by opening the gauche dihedral angle beyond 60°), but there is both computational and experimental support for the generality of this "gauche effect"²⁸ (and the related "anomeric effect"²⁹) between vicinal

**Figure 7.** INDO barrier potential of hydrazine (NH_2NH_2) as calculated with (—) and without (---) antibond orbitals, illustrating the strong gauche preference associated with the bond-antibond interactions of lone pairs.

L-polar bonds. Figure 8 shows the full INDO barrier potential (solid curve) for 1,2-difluoroethane, which yields the gauche conformer as the preferred form. By contrast, the barrier calculated from bond-bond interactions alone (dashed curve) shows only the strong electrostatic preference for the trans isomer, with no hint of the gauche minimum.

The tendency of vicinal lone pairs and L-polar bonds to adopt gauche conformations has been previously recognized, and christened the "gauche effect".²⁸ However, there is a slight ambiguity in the definition of the gauche effect as the "tendency to adopt that structure which has the maximum number of gauche interactions between the adjacent electron pairs and/or polar bonds".²⁸ While it is true that vicinal lone pairs or polar bonds prefer to be mutually gauche, we have seen (c) that a lone pair and a polar bond must generally prefer to be trans rather than gauche. For example, the molecule CF_2HNH_2 should prefer the gauche conformation (Table VIIa) rather than that (Table VIIb) which has the larger number of gauche interactions between the lone pair and the polar bonds.

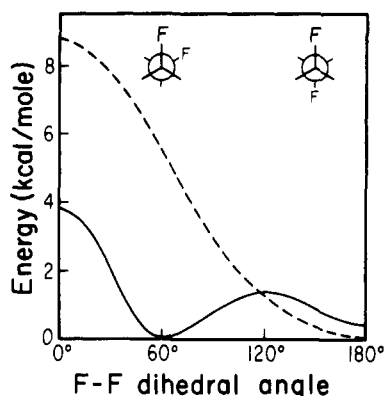


Figure 8. INDO barrier potential of 1,2-difluoroethane ($\text{CH}_2\text{FCH}_2\text{F}$) as calculated with (—) and without (---) antibond orbitals, illustrating the strong gauche preference associated with the bond-antibond interactions of polar bonds.

The simple conformational "rules" a-e listed above enable one to rationalize several of the important chemical trends in ethane-like molecules. Of course, these rules do not take the place of accurate SCF-MO (or CI) electronic structure calculations for more quantitative features of the barrier profiles.

VI. Relationship to Previous Work on Barrier Origins

While no attempt will be made to survey the extensive theoretical literature on rotation barriers, reference should be made to certain works that are closely related to the present treatment.³⁰

England and Gordon³¹ carried out extensive studies of INDO-SCF-MO rotation barriers by transforming canonical SCF-MOs to localized (LMO) form by the procedure of Edmiston and Ruedenberg.²² They concluded that the ethane barrier arises primarily from "interference" effects between the weak vicinal "tails" of incompletely localized CH bond orbitals. This conclusion is in accord with the general picture outlined above, where the important feature of CH bond delocalization was argued to be the weak mixing with vicinal antibonds. Inspection of the England-Gordon LMOs shows clearly the σ^* character of the "tails".

Our picture is also consistent with the PCILo calculations of Malrieu and co-workers.³² Although the PCILo (perturbative configuration interaction with localized orbitals) method lies outside the framework of MO theory, it employs a basis set of localized bond and antibond orbitals like those of our LCBO expansion, so that certain connections can be made. In particular, Malrieu et al. find that the barrier arises primarily from the set of singly excited determinants in which an occupied bond orbital of the principal determinant is replaced by the corresponding antibond orbital. Inasmuch as the primary effect of these single excitations is to correct the orbitals of the principal determinant, bringing them closer to SCF form, it is evident that such single excitations can be associated with the bond-antibond interactions of the present picture.

However, a somewhat different picture has emerged from bond-orbital wave functions built from nonorthogonal atomic hybrids. In a nonorthogonal basis there is no clear distinction between the contributions of "different" basis functions. In particular, a "bond orbital" of nonorthogonal hybrids can have significant overlap with orbitals on other atoms, such as the antibond orbitals at vicinal positions. In such a case, the determinantal product of nonorthogonal "bond orbitals" will implicitly bring in some of the bond-antibond interactions which (in an orthonormal basis) would appear to be of a different form. Indeed, to the extent that the overlap $S_{\sigma\sigma^*}$ of the nonorthogonal orbitals is proportional to the interaction ele-

ment $H_{\sigma\sigma^*}$, a simple perturbative estimate indicates that vicinal antibonds will be implicitly mixed into these "bond orbitals" by an amount which is comparable to their contribution to the occupied SCF-MOs. Thus, a determinantal product of nonorthogonal bond orbitals may give a reasonable rotation barrier even if no SCF procedure is employed.

Hoyland³³ showed that a determinantal product of bond orbitals $\tilde{\Omega}_i$ constructed from nonorthogonal hybrids gives a reasonable numerical barrier for ethane. A basic premise of that work is that there should be a close correspondence between the localized orbitals obtained from an SCF calculation and the symmetrically orthogonalized bond orbitals, i.e., that orthogonalization of the $\tilde{\Omega}_i$ builds in the "tails" noted by England and Gordon. Because the determinantal wave function

$$\tilde{\psi} = \det|\tilde{\Omega}_1 \tilde{\Omega}_2 \dots \tilde{\Omega}_N| \quad (6.1)$$

is invariant to the orthogonalizing transformation \mathcal{O}

$$\tilde{\Omega}_i \xrightarrow{\mathcal{O}} \tilde{\tilde{\Omega}}_i, \langle \tilde{\tilde{\Omega}}_i | \tilde{\tilde{\Omega}}_j \rangle = \delta_{ij} \quad (6.2)$$

up to a normalization constant, the antisymmetrizer has the indirect effect of orthogonalizing the $\tilde{\Omega}_i$'s. Note, however, that the subsequent orthogonalization (6.2) does not remove the bond-antibond mixing, so that Hoyland's numerical result is still consistent with our picture. In effect, there are two distinct ways of producing a set of orthonormal bond orbitals from a set of nonorthogonal AOs $\tilde{\chi}_\mu$, viz.

$$\tilde{\chi}_\mu \xrightarrow{\mathcal{O}} \chi_\mu \xrightarrow{\mathcal{B}} \Omega_i \quad (6.3a)$$

(orthog) (orthog)

$$\tilde{\chi}_\mu \xrightarrow{\mathcal{B}} \tilde{\Omega}_i \xrightarrow{\mathcal{O}} \tilde{\tilde{\Omega}}_i \quad (6.3b)$$

(nonorthog) (orthog)

(\mathcal{B} = transformation to bond orbitals, \mathcal{O} = orthogonalizer). A bond orbital from the set (6.3b) is a mixture of both bond and antibond orbitals from the set (6.3a).

Sovers et al.³⁴ carried out bond-orbital calculations similar to those of Hoyland, and compared the result with corresponding Hartree product (nonantisymmetrized) results, concluding that "the difference between the antisymmetrized and nonantisymmetrized bond model shows clearly the importance to the barrier of the restriction on the wavefunction introduced by the exclusion principle". This has also been interpreted as a form of "steric repulsion", and attributed to the "orthogonalizing effect" of the antisymmetrizer.³⁵ Our results indicate, however, that neither orthogonality nor antisymmetry can ensure a reasonable barrier if the bond-antibond interactions are omitted. Antisymmetrized wave functions constructed respectively from the bond orbitals (6.3a) or (6.3b)

$$\psi = \det|\Omega_1 \Omega_2 \dots \Omega_N| \quad (6.4a)$$

$$\tilde{\psi} = \det|\tilde{\tilde{\Omega}}_1 \tilde{\tilde{\Omega}}_2 \dots \tilde{\tilde{\Omega}}_N| \quad (6.4b)$$

though superficially similar, will nevertheless show quite different behavior with respect to the rotation barrier,³⁶ since the latter incorporates some of the bond-antibond mixing, whereas the former does not.

VII. Conclusion

A qualitative picture has been presented of the forces contributing to internal rotation barriers in ethane-like molecules, based on the LCBO analysis of INDO-SCF-MO theory. This picture can be understood in terms of elementary valence concepts, and permits simple predictions and rationalizations of conformational preferences and the associated chemical

trends. While the analysis derives from the INDO semiempirical framework, it is based on general features of the bond-antibond interactions that are expected to persist in other levels of molecular orbital theory. It would be interesting to know why INDO seems to systematically underestimate barriers, and what refinements are necessary for a more satisfactory picture of the barrier interactions. We are currently investigating these and other aspects of the LCBO analysis in an ab initio framework.

Acknowledgments. We thank Pat Carrick, Bob Weinstock, and Chris Corcoran for assistance in obtaining several of the tables and figures. Special thanks are due to Professor L. S. Bartell for encouragement (and patience) as this work was being brought to completion. Financial support of the Camille and Henry Dreyfus Foundation, the University of Wisconsin Graduate Research Committee, and the National Science Foundation is gratefully acknowledged. Portions of this work were completed while the authors were affiliated with Stanford University.

References and Notes

- (1) (a) Shell Development Co.; (b) University of Wisconsin—Madison.
- (2) (a) Kemp, J. D.; Pitzer, K. S. *J. Chem. Phys.* **1936**, *4*, 749. (b) For the historical background, see Orville-Thomas, W. J. In "Internal Rotation in Molecules", Orville-Thomas, W. J., Ed.; Wiley: New York, 1974; pp 1–18.
- (3) The following quotations are illustrative: "Despite the extensive studies which have been made on a large number of molecules, it is still true that the theory of the origin of these potential barriers is not very far advanced" (ref 4a). "While it is easy enough to show that the barrier is not due to these special effects, it is more difficult to sort out of the mass of information a simple explanation of what the barrier is due to" (ref 4b). "Despite the many theoretical papers published, no general agreement has yet been reached on an explanation for such barriers" (ref 6). "So far, these attempts have led to rather negative conclusions, that is, many effects have been found to be not responsible for the barrier, but it has not been possible to pinpoint a simple explanation of what causes the barrier" (ref 7).
- (4) (a) Wilson, E. B., Jr. *Adv. Chem. Phys.* **1959**, *2*, 367–393. (b) Cignitti, M.; Allen, T. L. *J. Phys. Chem.* **1964**, *68*, 1292–1297.
- (5) Lowe, J. P. *Prog. Phys. Org. Chem.* **1968**, *6*, 1–80.
- (6) Lowe, J. P. *Science* **1973**, *179*, 527–532.
- (7) Veillard, A. In ref 2b, pp 385–424.
- (8) Payne, P. W.; Allen, L. C. In "Modern Theoretical Chemistry", Vol. 4, "Applications of Electronic Structure Theory", Schaefer, H. F., Ed.; Plenum Press: New York, 1977; pp 29–108.
- (9) Pitzer, R. M.; Lipscomb, W. N. *J. Chem. Phys.* **1963**, *39*, 1995–2004.
- (10) See the many studies cited in ref 7 and 8. Formal arguments for the unimportance of correlation effects are given by Levy, B. L.; Moireau, M.-Cl. *J. Chem. Phys.* **1971**, *54*, 3316–3321.
- (11) Pople, J. A.; Beveridge, D. L. "Approximate Molecular Orbital Theory", McGraw-Hill: New York, 1970.
- (12) Radom, L.; Hehre, W. J.; Pople, J. A. *J. Am. Chem. Soc.* **1972**, *94*, 2371–2381.
- (13) See, e.g., Hoffmann, R. *J. Chem. Phys.* **1963**, *39*, 1397–1412. Pople, J. A.; Segal, G. A. *ibid.* **1965**, *43*, S136–149. Cambrion-Brüderlein, H.; Sandorfy, C. *Theor. Chim. Acta* **1966**, *4*, 224–235. Gordon, M. S. *J. Am. Chem. Soc.* **1969**, *91*, 3122–3130. Bodor, N.; Dewar, M. J. S.; Harget, A.; Haselbach, E. *ibid.* **1970**, *92*, 3854–3859.
- (14) Pullman, B., Ed. "Quantum Mechanics of Molecular Conformations", Wiley: New York, 1976. See particularly the articles by Fernandez-Alonso, Christoffersen, and Pullman.
- (15) Ewig, C. S.; Van Wazer, J. R. *J. Chem. Phys.* **1976**, *65*, 2033–2036.
- (16) Stevens, R. M. *J. Chem. Phys.* **1970**, *52*, 1397–1402.
- (17) Pople, J. A.; Gordon, M. J. *Am. Chem. Soc.* **1967**, *89*, 4253–4261.
- (18) Allen, L. C. *Chem. Phys. Lett.* **1968**, *2*, 597–601.
- (19) Brunck, T. K.; Weinhold, F. *J. Am. Chem. Soc.* **1976**, *98*, 4392–4393.
- (20) Weinhold, F.; Brunck, T. K. *J. Am. Chem. Soc.* **1976**, *98*, 3745–3749.
- (21) Brunck, T. K.; Weinhold, F. "Linear-Combination-of-Bond-Orbitals Approach to SCF-MO Theory", University of Wisconsin Theoretical Chemistry Institute Report WIS-TCI-560 (unpublished).
- (22) Edmiston, C.; Ruedenberg, K. *Rev. Mod. Phys.* **1963**, *35*, 457–465. Boys, S. F. In "Quantum Theory of Atoms, Molecules, and the Solid State", Löwdin, P.-O., Ed.; Academic Press: New York, 1966.
- (23) See e.g., Hoffmann, R. *Acc. Chem. Res.* **1971**, *4*, 1–9.
- (24) Weiss, S.; Lerol, G. E. *J. Chem. Phys.* **1968**, *48*, 962–967.
- (25) Lowe, J. P. *J. Am. Chem. Soc.* **1970**, *92*, 3799–3800.
- (26) The corresponding overlap integrals $S_{\sigma\sigma^*}$ are 0.073 for the trans arrangement and 0.025 for the cis (opposite signs). One can picture the negative lobe of the antibond as "canceling out" some of the favorable interaction when the two orbitals lie in the cis orientation.
- (27) We use the gauche or trans designation to specify the conformation in terms of the "unique" element of each rotor—in this case, the CF bond and the nitrogen lone pair.
- (28) Wolfe, S. *Acc. Chem. Res.* **1972**, *5*, 102–111, and references cited therein.
- (29) See, e.g., Eliel, E. L.; Giza, C. A. *J. Org. Chem.* **1968**, *33*, 3754–3758.
- (30) In addition to works discussed more completely below, our treatment also bears some relationship to the recent "group orbital" analysis of Whangbo et al. (Whangbo, M.-H.; Schlegel, H. B.; Wolfe, S. *J. Am. Chem. Soc.* **1977**, *99*, 1296–1304), to Lowe's (ref 6) analysis in terms of asymmetrical splitting of interacting nonorthogonal orbitals, and to various discussions of "hyperconjugative effects", "back-donation", and so forth (see, e.g., ref 12). For example, the splitting asymmetry discussed by Lowe, which seems a type of "overlap effect" in a nonorthogonal basis, would appear as a bond-antibond interaction in an orthogonal basis, these two descriptions being fully consistent with one another. Since this work was first carried out (Brunck, T. K. Ph.D. Thesis, Stanford University, 1976), a monograph appeared (Epitotis, N. D.; Cherry, W. R.; Shaik, S.; Yates, R. L.; Bernardi, F. *Top. Curr. Chem.* **1977**, *70*) in which similar conclusions are drawn concerning the importance of bond-antibond interactions in configurational stability. Although their analysis proceeds from quite different assumptions, and differs from ours in certain respects (such as the relative importance of "energy control" and "matrix element control" of the interactions), there is agreement on basic features of the bond-antibond interactions, which we regard as important support for the validity of the general picture sketched here. We thank Professor E. R. Davidson for bringing this reference to our attention.
- (31) England, W.; Gordon, M. S. *J. Am. Chem. Soc.* **1971**, *93*, 4649–4657. *Ibid.* **1972**, *94*, 4818–4823, and subsequent papers.
- (32) Diner, S.; Malrieu, J. P.; Jordan, F.; Gilbert, M. *Theor. Chim. Acta* **1969**, *15*, 100–110. Malrieu, J. P. In "Modern Theoretical Chemistry", Vol. 7, "Semiempirical Methods of Electronic Structure Calculations", Segal, G. A., Ed.; Plenum Press: New York, 1977; pp 69–103.
- (33) Hoyland, J. R. *J. Am. Chem. Soc.* **1968**, *90*, 2227–2232. *J. Chem. Phys.* **1969**, *50*, 473–478. See also Musso, G. F.; Magnasco, V. *ibid.* **1974**, *60*, 3754–3759.
- (34) Sovers, O. J.; Kern, C. W.; Pitzer, R. M.; Karplus, M. *J. Chem. Phys.* **1968**, *49*, 2592–2599. Kern, C. W.; Pitzer, R. M.; Sovers, O. J. *ibid.* **1974**, *60*, 3583–3587. Stevens, R. M.; Karplus, M. *J. Am. Chem. Soc.* **1972**, *94*, 5140–5141.
- (35) See, e.g., Christiansen, P. A.; Palke, W. E. *Chem. Phys. Lett.* **1975**, *31*, 462–466. Payne, P. W.; Allen, L. C. *J. Am. Chem. Soc.* **1977**, *99*, 3787–3794. Reference 6.
- (36) We have recently confirmed this difference by an ab initio calculation for ethane; a determinantal function constructed as in (6.4a) gives a barrier of only 0.5 kcal/mol, whereas the corresponding Hoyland-like function (6.4b) gives 3.2 kcal/mol. Full details of this calculation will be reported elsewhere (Corcoran, C. T.; Weinhold, F. In preparation).